Study of equilibrium beach profiles

Article · January 1976

DOI: 10.9753/icce.v15.74

2 authors, including:

Robert Anthony Dalrymple
Johns Hopkins University
290 PUBLICATIONS **11,515** CITATIONS

SEE PROFILE

CHAPTER 75

STUDY OF EQUILIBRIUM BEACH PROFILES

by

Robert A. Dalrymple[1] and William W. Thompson[2]

Abstract

The use of the dimensionless fall velocity for determining equilibrium foreshore slopes, modeling of natural beaches in the laboratory, and for determining shoreline erosion rates is examined. Encouraging results are found for relating foreshore slope uniquely to the dimensionless fall velocity and possible model law is proposed.

Introduction

At the University of Delaware, work has been progressing on the development of computer models for nearshore processes and coastal modification (Wang, Dalrymple and Shiau, 1975; Birkemeier and Dalrymple, 1975). During the course of the work it was necessary to be able to predict equilibrium beach slopes, based not only on the grain size of the material that comprised the beach as was done by Bascom (1951), but also as a function of the incident wave characteristics. Work of this nature has been conducted previously by Kemp (1968), Nayak (1970) and Carter, Mei and Liu (1973). This paper presents the foreshore slope as a function of the dimensionless fall velocity of the sediment, a parameter introduced by Nayak on dimensional grounds and by Dean (1973), based on a physical argument.

Based on the success of the dimensionless fall velocity as a measure of the beach slope and also as an indicator of the reflection from the beach (see Nayak, 1970), numerous model laws were developed for the modeling of beaches in the laboratory, keeping the dimensionless fall velocity ratio constant. Several of these relationships were tested in the laboratory and compared against prototype data in the same manner as Noda (1972) and Paul, Kamphuis and Brebner (1972).

[1]Assistant Prof., Dept. of Civil Engineering, Univ. of Delaware, Newark, DE 19711.

[2]Formerly, Graduate Student, Univ. of Delaware, now with Transworld Drilling Co., Morgan City, La.

XV ICCE
1976

A major area of coastal engineering that is still not adequately understood is onshore-offshore sediment transport. From the laboratory tests mentioned above, a speculative empirical relationship is presented for foreshore erosion/deposition based again on the dimensionless fall velocity, which has been shown to be an indication of when erosion or deposition will take place.

Equilibrium Beach Profile and Foreshore Slope

Equilibrium profiles have been studied extensively through the history of coastal engineering, and as early as 1939, Waters postulated that the type of profile (that is, whether a normal profile, with steep foreshore slope and possibly a step at the breaker line, or a bar profile, with a milder foreshore slope and a longshore bar at the breaker line) was determined by the deep water steepness, H_o/L_o, the ratio of the deep water values of the wave height and wave length. For many years it has been held as a basic tenet that $H_o/L_o = 0.025$ is the dividing wave steepness between profile types with barred profiles resulting from steeper waves, despite some evidence to the contrary (e.g., Saville, 1957; King, 1972). In 1973, Dean found that the wave steepness separating bar profiles from normal profiles varied with the fall velocity of the sediment, V_f, divided by the deepwater celerity, $C_o = L_o/T$, where T is the wave period.

$$\frac{H_o}{L_o} = 0.85 \frac{V_f}{C_o}$$

which can be written as $H_o/V_fT = 0.85$. The fall velocity was calculated using the median grain size, d_{50}. Kohler and Galvin (1973) using different data recommended, $H_o/V_fT = 0.70$, while the CERC Shore Protection Manual (1973) recommends 1.0 - 2.0.

The physical significance of the dimensionless fall velocity, H_o/V_fT, as presented by Dean is that the parameter is a measure of whether a particle lifted into suspension by the passage of a wave can fall to the bottom during the time when its net displacement due to the horizontal water particle motion is shoreward. If so, the net sediment transport in the surf zone is shoreward, or zero, and we expect a summer profile to develop or to have been developed. Also the parameter can be viewed as the tangent/π of the angle made by the maximum horizontal velocity in deepwater and the fall velocity.

If the parameter, H_o/V_fT, is an important parameter for profile type, it follows (by dimensional analysis) that it is also important for determination of the foreshore slope, θ, measured in degrees at the still water line. Collecting data from different experimenters, including Rector (1954), Fairchild (1959), Raman and Earattupuzha (1972), van Hijum (1974) and Thompson (1976), foreshore slopes were measured and are presented in Fig. 1 versus the dimensionless fall velocity. The figure shows a reasonable trend despite the significant scatter which could be attributed to any number of things including inaccuracy in our

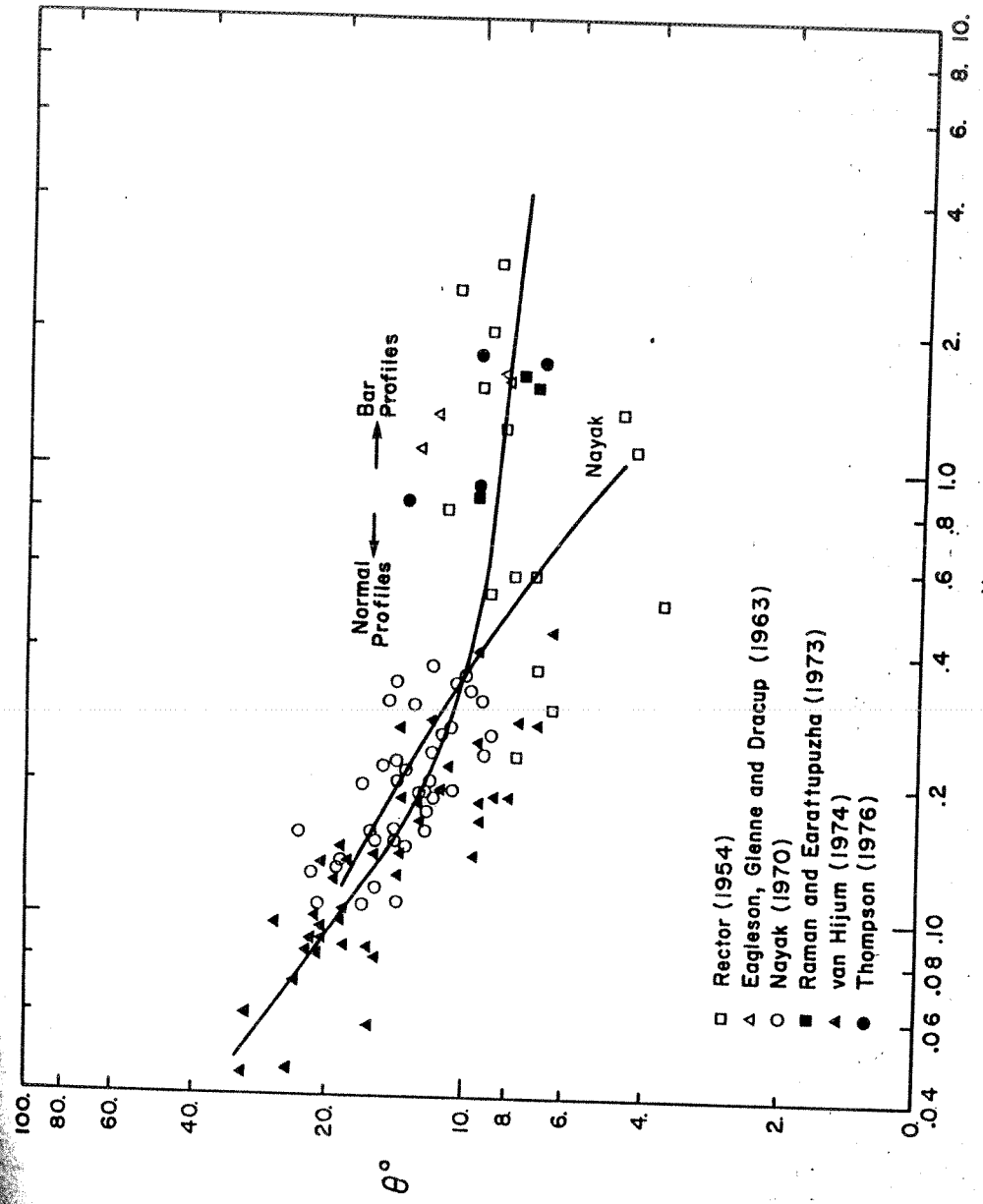

Figure 1 Foreshore Beach Slope Versus Dimensionless Fall Velocity

measurement of θ from the experimenter's figures, profile measurement errors, lack of equilibrium[3] and spurious tank reflections. The scatter, however, is less than was obtained by attempting to plot the data versus H_o/L_o with a third parameter, such as d_{50}/H_o, d_{50}/L_o and C_o/V_f.

Nayak's(1970) curve is also shown in the figure, but only over the range for which he used quartz sand. When he used much lighter material, his beach slopes became very mild and, in fact, the whole beach itself was in motion with the waves. Also Kemp (1968) has plotted θ versus a dimensional parameter, $H_b/Td_{50}^{1/2}$, which is similar to the dimensionless fall velocity as V_f is directly proportional to $d_{50}^{1/2}$ for large sand sizes. Ours appears to be significantly different from his, particularly for larger values of H_o/V_fT.

Modeling Relationships

From Fig. 1, which indicates a unique foreshore slope for a given value of H_o/V_fT, it follows that in order to reproduce in a model the same equilibrium profile that occurs in the prototype (neglecting tidal effects) that the parameter H_o/V_fT should be the same in model and prototype. Based on different modeling requirements seven model laws were developed and are presented in Table 1. The derivations are shown in the Appendix.[4] Four of the model laws (#3,5,6,7) accommodate the same sand in model and prototype and were tested in the laboratory. However, of these, only #7 maintains geometric similarity (that is, the horizontal length scale, λ, is equal to the vertical length scale, μ), and, therefore, only it should yield a corrected modeled beach slope, while it was hoped that the others might adequately model other features of the profile.

Experiments were conducted in a 21.3 m long x 0.61 m wide wave tank with a piston wavemaker at one end and the sand beach at the other. The experimental program was to run prototype tests for a normal and barred profile and then to model these with tests based on the model laws. The beach material consisted of a quartz sand with a median diameter, d_{50} of 0.40 mm (a Trask sorting coefficient of 1.38 and a skewness of 1.0). Due to tank size restrictions, the maximum practical scaling was only $\mu = 1/2$. Most of the tests were initiated with a plane profile (1:10 for the prototype tests) and allowed to run to equilibrium which was defined as a lack of significant profile change with time in the foreshore region. For the foreshore region,

---

[3] Chesnutt and Galvin (1974) report never achieving equilibrium in their tests despite holding H_o/L_o constant as the air temperature and hence H_o/V_fT changed.

[4] The derivation of the model laws utilized the Stokes equation for fall velocity which is valid only for low Reynolds numbers. For larger Reynolds numbers, a different fall velocity relationship is necessary and, in fact, for Model Laws 1 and 2, it is only necessary to scale the fall velocity as $\mu^{1/2}$ and then choose the sand size accordingly.

TABLE 1 SUMMARY OF MODEL LAWS
(See Appendix A for Derivation)

Law	$n_{\gamma'}$	$n_{d_{50}}$	n_T	λ	Note
1	1	$\mu^{1/4}$	$\mu^{1/2}$	μ	Preserves Froude No., H_o,L_o, geometric similarity, Stokes fall velocity
2	$\mu^{3/2}$	$\mu^{-1/2}$	$\mu^{1/2}$	μ	Preserves bed particle Reynolds number, densimetric Froude number, H_o/L_o.
3	1	1	μ	$\mu^{3/2}$	Assumes laminar boundary layer. Preserves bed shear stress, Froude No.
4	$\mu^{-0.1875}$	$\mu^{+0.063}$	$\mu^{1.0625}$	$\mu^{1.5625}$	Assumes turbulent boundary layer.
5	1	1	μ	$\mu^{3/2}$	Preserves Froude No.
6	1	1	μ	μ^2	Preserves bed particle Reynolds number, bed shear stress.
7	1	1	μ	μ	Preserves geometric similarity, H_o/L_o.

$$n_{\text{parameter, a}} = \frac{a_{\text{model}}}{a_{\text{prototype}}}$$

$$\gamma' = \frac{\gamma_{\text{sediment}} - \gamma_{\text{fluid}}}{\gamma_{\text{fluid}}}$$

d_{50} = median grain size diameter

T = wave period

λ = horizontal length scale

μ = vertical length scale

the foreshore slope and the related profile was achieved quickly, in the matter of several hours; however, the offshore region, dominated by migratory ripples, equilibrium took much longer to achieve, particularly for the barred profile.

A summary of the tests is presented in Table 2, including the initial variables and the time to equilibrium, t_e. The resulting model beach profiles obtained for the different model laws (note that #3 and 5 have the same scaling relationships despite different assumptions) were scaled up to prototype scale and plotted with a common still water line intersection. The results are shown in Figs. 2 and 3 for the normal and barred profiles. As can be seen

TABLE 2 EXPERIMENTAL TEST VALUES

	i	d(in)	H(in)	Ho(in)	T(sec)	Temp.(°C)[1]	V_f(in/sec)	H_o/L_o	H_o/V_fT	t_e(hrs)
Prototype										
Summer	1:10	27.0	4.00	4.28	2.1	13.5	2.20	.0158	.928	21
Winter	1:10	27.0	7.50	8.05	2.1	14.0	2.20	.0297	1.745	18.5
Model Law #7										
Summer	1:10	13.5	2.00	2.18	1.05	22.0	2.44	.0323	.850	12
Winter	1:10	13.5	3.75	4.09	1.05	14.5	2.24	.0605	1.740	15
Model Laws #3, #5										
Summer	1:7	13.5	2.00	2.18	1.05	25.0	2.52	.0323	.825	8
Winter	1:7	13.5	3.75	4.09	1.05	25.5	2.52	.0605	1.540	11
Model Law #6										
Summer	1:5	13.5	2.00	2.18	1.05	23.0	2.44	.0323	.850	*(24)
Winter	1:5	13.5	3.75	4.09	1.05	14.0	2.20	.0605	1.760	*(18.5)

[1]Median water temperature

*Test Time, did not attain equilibrium

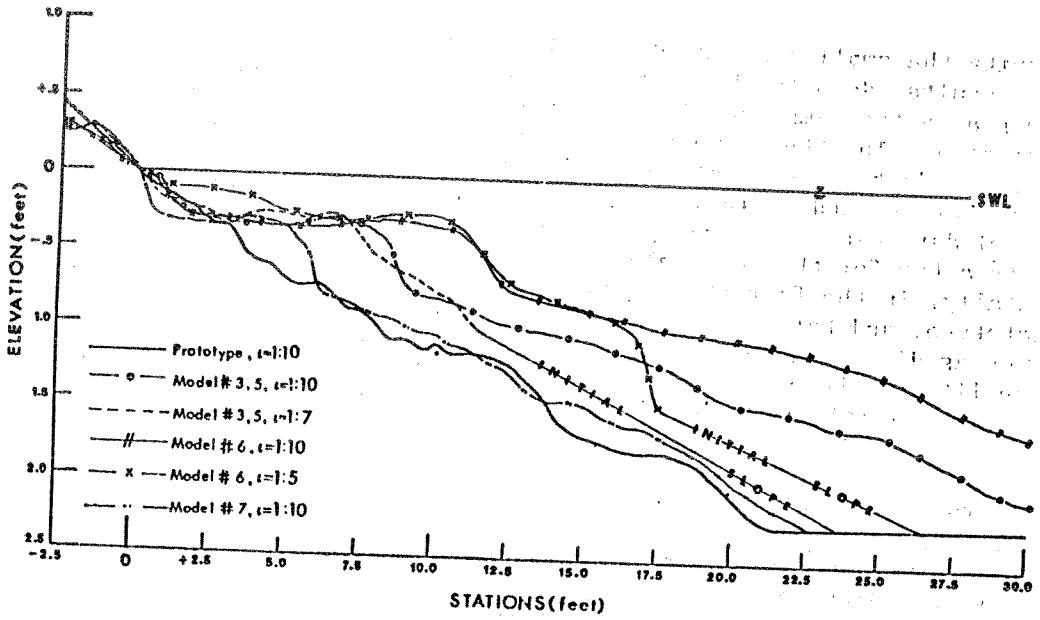

Figure 2 Comparison of Model Laws for Normal Profile. Station 0 = Intersect of SWL and Equilibrium Profile

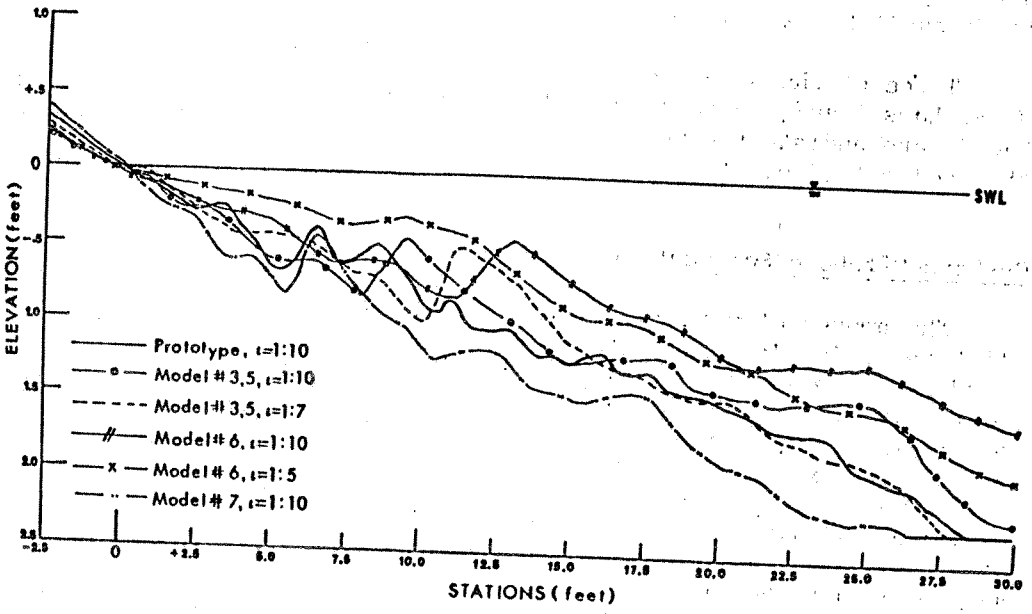

Figure 3 Comparison of Model Laws for Barred Profile. Station 0 = Intersect of SWL and Equilibrium Profile

despite the small scaling ($\mu = 1/2$), there are wide discrepancies in the results, despite the fact that the dimensionless fall velocity was nearly the same (varying due to temperature effects on the fall velocity). The "best" model law of the four tested appears to be #7, as it predicted the location of the primary bar for the steep waves (bar profile) and it follows the normal profile reasonably well for the milder waves. A discrepancy occurs in the model in that it predicts a bar for this case also, however, the problem lies (experimentally) in the fact that H_o/V_fT differs slightly between model and prototype, and both values are near the transition line between profile types as discussed in the first section. The primary reason for the inability of the other models to predict the prototype equilibrium profile appears to be the distortion of these models.

The only difference between the four models is the length scale and, therefore, only the initial slopes were varied to start each test. Comparing the model test results prior to scaling to prototype gives an indication of the effect of initial slope on final profile. Fig. 4 shows the results for the normal profiles. In the onshore region the initial slope makes no difference at all, and, thus, has no effect on the foreshore slope. However, in the offshore region it is important as it is a measure of the amount of sand available to be moved by the waves. For model tests where the depth of water at the toe of the beach is deeper than the depth at which material is moved by the waves then the initial slope will have no effect on the final equilibrium profile.

Three of the proposed models' laws were not tested. Of them, Model Laws 1 and 2 appear to be better ones in that they, like Model Law 7, are undistorted models. As Model Law 1 only requires modeling the sediment size, it appears to be the most practical.

Onshore-Offshore Sediment Transport

The amount of material transported between the foreshore and the offshore region is of importance for beach erosion considerations. Based on dimensional analysis, an erosion parameter, $Q/H_o di$, was chosen to represent this volumetric transport. The variable, Q, is the volume of material per unit width of tank eroded or deposited onshore of the breaker line and di, the product of the depth of water at the toe of the beach and the initial beach slope is a measure of the amount of material in the tank. The initial slope, i, is also important as the erosion or deposition in the onshore zone depends on whether or not the initial slope is greater than or less than the equilibrium slope. The results which are extremely speculative are shown in Fig. 5. Clearly more data is necessary to verify if the form of the curve is correct.

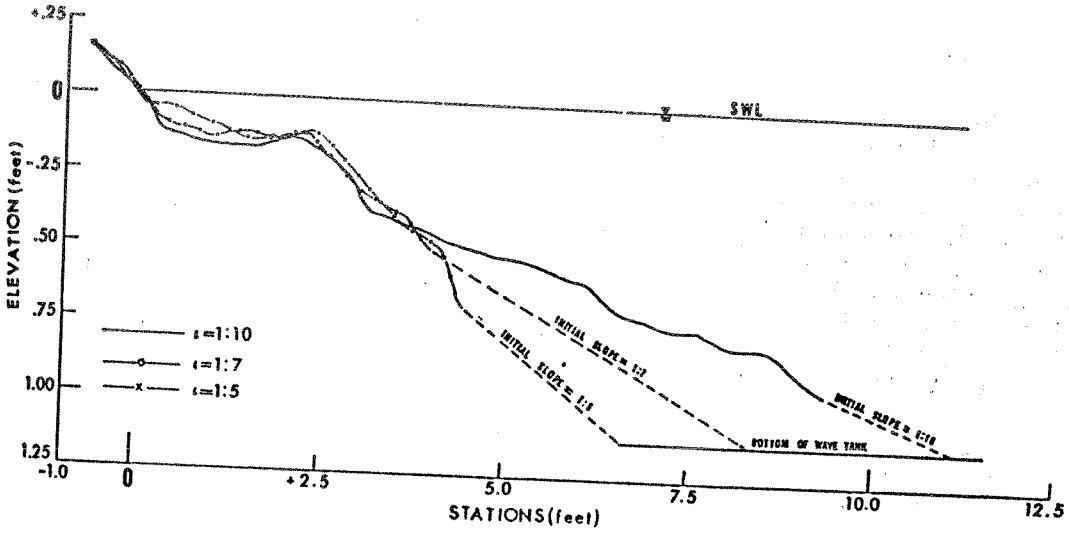

Figure 4 Comparison of Initial Slopes for Normal Profile

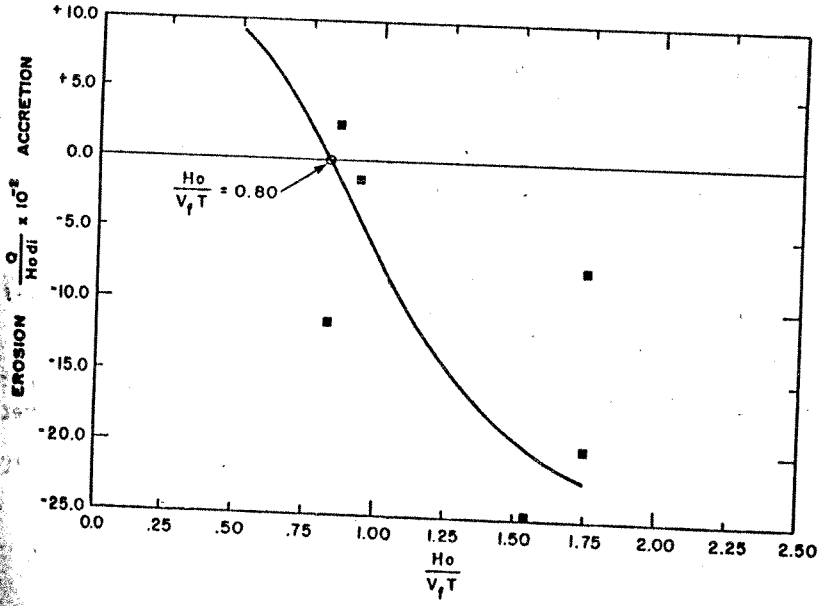

Figure 5 Inshore Erosion Versus Dimensionless Fall Velocity

Conclusions

The foreshore slope angle is uniquely related to the nondimensional parameter H_o/V_fT which accounts for the major wave and material properties. For mild waves, the beach slope will be steeper than for steeper waves. Based on experimental results, the slope is independent of initial conditions and can be repeated for similar laboratory conditions. The slope is also a very important characteristic feature of the application to natural beaches as the region inshore of the breaker line is the region of most concern to the users of the beach. The slope angle is relatively easy to identify and measure in the field as compared to the identification of an offshore bar.

A model law preserving the parameter, H_o/V_fT has not been proven experimentally although Model Law #1 apparently includes the most important assumptions. Based on the experimental verification of four of the proposed model laws, the model should be geometrically similar to the prototype and should preserve the wave steepness ratio and the parameter, H_o/V_fT. To preserve both the wave steepness ratio and H_o/V_fT, the material size must also be modeled and the same material used in the model and prototype to eliminate the alien effects of lightweight materials.

References

Bascom, W.J., "The Relationship Between Sand Size and Beach-Face Slope," Trans., Amer. Geophys. Union, Vol. 32, No. 6, 1951.

Birkemeier, W.A. and R.A. Dalrymple, "Nearshore Water Circulation Induced by Wind and Waves," Proc. Symp. on Modeling Tech., ASCE, San Francisco, 1975.

Carter, T.G., Liu, P. L-F. and C. C. Mei, "Mass Transport by Waves and Offshore Bed Forms," J. Waterways, Harbors and Coastal Engrg., ASCE, Vol. 99, No. WW2, May, 1973.

Chesnutt, C.B. and C.J. Galvin, "Lab Profile and Reflection Changes for H_o/L_o = 0.02," Proc. 14th Conf. on Coastal Engrg., ASCE, Vancouver, 1974.

Dean, R.G., "Heuristic Models of Sand Transport in the Surf Zone," Proc. Conf. on Engrg. Dynamics in the Surf Zone, Sydney, May, 1973.

Eagleson, P.S., Glenne, B. and J.A. Dracup, "Equilibrium Characteristics of Sand Beaches," J. Hyd. Div., ASCE, No. HY1, Jan., 1963. See also U.S. Army Beach Erosion Board Tech. Memo. 126, July, 1961.

Fairchild, J.C., "Suspended Sediment Sampling in Laboratory Wave Action," U.S. Army Beach Erosion Board Tech. Memo. 115, June, 1959.

Henderson, F.M., Open Channel Flow, MacMillan Company, New York, 1966.

References (Continued)

Jonsson, I.G., "Wave Boundary Layers and Fraction Factors," Proc. of 10th Conf. on Coastal Engrg., ASCE, London, 1966.

Kamphuis, J.W., "Short Wave Models with Fixed Bed Boundary Layers," J. Waterways, Harbors and Coastal Engrg., ASCE, No. WW4, 1973.

Kemp, P.H., "Beaches Produced by Waves of Low Phase Difference," J. Hyd. Div., ASCE, No. HY 5, Sept., 1968.

King, C.A.M., Beaches and Coasts, 2nd Ed., St. Martins Press, New York, 1972.

Kohler, R.R. and C.J. Galvin, "Berm-Bar Criterion," unpublished Memorandom for the Record, U.S. Army CERC, Washington, Aug.,

LeMehaute, B., "A Comparison of Fluid and Coastal Similitude," Proc. of the 12th Coastal Engrg. Conf., Washington, 1970.

Nayak, J.V., "Equilibrium Profile of Model Beaches," Doctoral Dissertation, Univ. of Calif., at Berkeley, June, 1970.

Noda, E.K., "Equilibrium Beach Profile Scale-Model Relationships," J. Waterways, Harbors and Coastal Engrg., ASCE, No. WW4, Nov., 1972.

Paul, M.J., Kamphuis, J.W. and A. Brebner, "Similarity of Equilibrium Beach Profiles," Proc. 13th Coastal Engrg. Conf., ASCE, Vancouver, 1972.

Raman, H. and J.J. Earattupuzha,"Equilibrium Conditions in Beach Wave Interaction," Proc. 13th Coastal Engrg. Conf., ASCE, Vancouver, 1972.

Rector, R.L., "Laboratory Study of Equilibrium Profile of Beaches," U.S. Army B.E.B.T.M. 41, Aug., 1954.

Saville, T., "Scale Effects in Two Dimensional Beach Studies," Trans. Int. Assoc. of Hyd. Res., 7th General Meeting, 1957.

Thompson, W.W., "A Study of Equilibrium Beach Profiles," M.C.E. Thesis, Univ. of Delaware, June, 1976.

U.S. Army Coastal Engineering Research Center, Shore Protection Manual, Washington, DC, 1973.

van Hijum, E.,"Equilibrium Profiles of Course Material Under Wave Attack," Proc. 14th Coastal Engrg. Conf., ASCE, Copenhagen, 1974, also personal communication, 1976.

Wang, H., Dalrymple, R.A. and J.C. Shiau, "Computer Simulation of Beach Erosion and Profile Modification Due to Waves," Proc. Symp. on Modeling Tech., ASCE, San Francisco, 1975.

References (Continued)

Waters, C.H., "Equilibrium Studies of Sea Beaches," M.S. Thesis, Univ. of California at Berkeley, 1939.

APPENDIX A

DEVELOPMENT OF EQUILIBRIUM PROFILE MODEL LAWS

To completely define the following model laws, the horizontal scale, the median grain diameter, the submerged specific weight of the beach material and the time scale will be expressed in terms of the vertical scale. As only equilibrium profiles are considered, the time to equilibrium is not modeled. The variable H_o/V_fT will be preserved in all model laws. Further, the scale ratio of a parameter $n_{parameter}$, equals the ratio of the parameter in the model to the same parameter in the prototype. The following notation will be incorporated in the derivations:

$$n_{\text{vertical length}} = \mu$$

$$h_{\text{horizontal length}} = \lambda$$

$$n_{\text{time scale}} = n_T$$

$$n_{\text{median grain diameter}} = n_{d_{50}}$$

$$n_{\text{sediment relative specific weight}} = n_{\gamma'}$$

where $\gamma' = \dfrac{\gamma_{\text{sediment}} - \gamma_{\text{fluid}}}{\gamma_{\text{fluid}}}$.

The resulting model relations are summarized in Table 1.

1. Model Law #1

The deepwater wave steepness, H_o/L_o, has been shown to be a governing factor in the shaping of beach profiles. Preserving H_o/L_o and defining $n_{H_o} = \mu$ and $n_{L_o} = \lambda$,

$$\mu = \lambda \tag{1.1}$$

Modeling the deepwater wave length, $L_o = g/2\pi\ T^2$, or requiring Froude similitude

$$n_T = \mu^{1/2} \tag{1.2}$$

From Equation 1.2, the modeling of H_o/V_fT yields $\mu = n_{V_f}\ \mu^{1/2}$ or

$$n_{V_f} = \mu^{1/2} \tag{1.3}$$

This defines a model law in terms of n_{V_f}, n_T, μ, λ. The scale parameter $n_{d_{50}}$, may be obtained from curves of V_f versus d (see, e.g., Shore Protection Manual).

For low Reynolds numbers, the Stokes equation for the sediment fall velocity is

$$V_f = \frac{1}{18}\frac{d_{50}^2\ g\ \gamma'}{\nu} \tag{1.4}$$

Preserving the Stokes equation and using the same fluid in the model and the prototype, $n_\nu = 1$,

$$n_{V_f} = n_{d_{50}}^2\ n_{\gamma'} \tag{1.5}$$

For the same material in the model and the prototype, $n_{\gamma'} = 1$, Equation (1.5) reduces to upon substitution of Equation (1.3),

$$n_{d_{50}} = \mu^{1/4} \tag{1.6}$$

2. Model Law #2

Eagleson, Glenne and Dracup (1963) concluded that the equilibrium profile shape is a function of the incipient point for sediment movement. This point is determined by the relative magnitudes of the sediment weight and the bed shear stress. A nondimensional ratio of the gravitational force and the shear stress, the densimetric Froude number is defined as $F_* = \mu_*/(g\gamma'\ d_{50})^{1/2}$. Modeling F_*,

$$n_{\mu_*}^2 = n\ ,\ n_{d_{50}} \tag{2.1}$$

Preserving the bed particle Reynolds number which is defined as $R_{e_s} = \mu_*.d_{50}/\nu$ and using the same fluid in the model and the prototype,

$$n_{\mu_*} = \frac{1}{n_{d_{50}}} \tag{2.2}$$

Simplifying Equation 2.2 by means of Equation 2.1,

$$n_{\gamma'} = \frac{1}{n_{d_{50}}^3} \tag{2.3}$$

Preserving the Froude number, $F = V/(gd)^{1/2}$,

$$n_V = \mu^{1/2} \tag{3.5}$$

Upon the substitution of $n_V = \mu^{1/2}$ in Equation 3.4,

$$n_{u_*} = \mu^{1/4}\, n_T^{-1/4} \tag{3.6}$$

Modeling the bed particle Reynolds number, $n_{u_*} = 1/n_{d_{50}}$, Equation 2.2,

$$n_{d_{50}} = \mu^{-1/4}\, n_T^{1/4} \tag{3.7}$$

From the modeling of the densimetric Froude number, $n_{u_*}^{\ 2} = n_{\gamma'}\, n_{D_{50}}$, Equation 2.1,

$$n_{\gamma'} = \frac{\mu^{3/4}}{n_T^{3/4}} \tag{3.8}$$

upon the substitution of the expressions for n_{u_*}, Equation 3.6 and $n_{d_{50}}$, Equation 3.7. For the same material in the model and the prototype, $n_{\gamma'} = 1$, $n_T = \mu$. Preserving H_o/V_fT, $n_{V_f} = 1$ and subsequently, $n_{d_{50}} = 1$. A kinematic condition proposed by LeMehaute (1970) stipulates that the ratio of the horizontal, V, and vertical velocity, V_f, be scaled as the ratio of the length scales, λ and μ, $n_V/n_{V_f} = \lambda/\mu$. For $n_V = \mu^{1/2}$, Equation 3.5,

$$\lambda = \mu^{3/2} \tag{3.9}$$

4. Model Law #4

Assuming a turbulent boundary layer, the friction factor is defined by Kamphuis (1973) as

$$f = .47\, \left(\frac{k_s}{a_\delta}\right)^{3/4} . \tag{4.1}$$

Modeling f,

$$n_f = n_{k_s}^{\ 3/4}\, n_{a_\delta}^{\ -3/4} \tag{4.2}$$

The term a_δ is defined as the wave orbital amplitude at the top of the boundary layer. For shallow water waves, the orbital amplitude equals

$$\delta = \frac{HT}{4\pi}\sqrt{\frac{g}{d}} . \tag{4.3}$$

The scale factors λ and n_T are modeled similarly in accordance with Equations 1.1 and 1.2 for the modeling of H_o/L_o. By modeling of H_o/V_fT,

$$n_{V_f} = \mu^{1/2} \tag{2.4}$$

Again a model law now exists for the general case with $n_{d_{50}}$ determined from the V_f-d_{50} curve. In this case the same material could even be used in model and prototype provided a different fluid or possibly different temperature is used. For low Reynolds numbers modeling the Stokes equation for fall velocity, $n_{V_f} = n_{d_{50}}{}^2 \gamma'$,

$$n_{d_{50}} = \mu^{-1/2} \tag{2.5}$$

and

$$n_{\gamma'} = \mu^{3/2} \tag{2.6}$$

upon substitution of Equations 2.3 and 2.4. For this model law, both the sediment specific weight and the size are modeled.

3. Model Law #3

Assuming a laminar boundary layer, the bed shear stress for incipient motion will be formulated differently from Model Law #2 based on the definition of the bed friction factor. The friction factor for a laminar boundary layer for gravity wave flow is expressed by Jonsson (1966) as

$$f = \sqrt{\frac{\pi}{2}} \frac{\nu^{1/2}}{V\sqrt{T}} \tag{3.1}$$

Modeling f and assuming the same fluid in the model and the prototype,

$$n_f = n_V{}^{-1} n_T{}^{-1/2} \tag{3.2}$$

Henderson (1966) defined the bed shear velocity, u_*, as

$$u_* = \frac{f^{1/2}}{\sqrt{8}} V \tag{3.3}$$

Modeling u_* and simplifying per the Equation 3.2 for n_f,

$$n_{u_*} = n_V{}^{1/2} n_T{}^{-1/4} \tag{3.4}$$

Modeling a_δ,

$$n_{a_\delta} = \mu^{1/2}\, n_T \tag{4.4}$$

The term k_s is defined as the bottom sand grain roughness and is assumed proportional to the median grain diameter. Defining the scale ratio os k_s as $n_{k_s} = n_{d_{50}}$ and incorporating the relations for n_{k_s} and n_{a_δ}, the expression for n_f, Equation 4.2, reduces to

$$n_f = \frac{n_{d_{50}}^{3/4}}{\mu^{3/8}\, n_T^{3/4}} \tag{4.5}$$

Modeling the bed shear velocity, $u_* = (f^{1/2}/\sqrt{8})\, V$, as previously defined by Henderson (1966),

$$n_{u_*} = n_f^{1/2}\, n_V \quad . \tag{4.6}$$

Preserving the Froude number, $n_V = \mu^{1/2}$, n_{u_*} simplifies to

$$n_{u_*} = \frac{\mu^{5/16}\, n_{d_{50}}^{3/8}}{n_T^{3/8}} \tag{4.7}$$

upon the substitution of the equations for n_V and n_f. Preserving the bed particle Reynolds number, $n_{u_*} = 1/n_{d_{50}}$, n_{u_*} reduces to

$$n_{d_{50}} = \frac{n_T^{3/11}}{\mu^{5/22}} \tag{4.8}$$

Using the equations, $n_{u_*} = 1/n_{d_{50}}$ which preserves the bed particle Reynolds number and $n_{u_*}^2 = n_{\gamma'}\, n_{d_{50}}$ which preserves the densimetric Froude number,

$$n_{\gamma'} = \frac{1}{n_{d_{50}}^3} \tag{4.9}$$

Modeling the Stokes equation for the fall velocity, $n_{V_f} = n_{d_{50}}^2\, n_{\gamma'}$,

$$n_{V_f} = \frac{1}{n_{d_{50}}} \quad , \tag{4.10}$$

per the substitution of $n_{\gamma'}$, Equation 4.9. Expressing n_{V_f} in terms of $n_{d_{50}}$, Equation 4.8,

$$n_{V_f} = \frac{\mu^{5/22}}{n_T^{3/11}} \tag{4.11}$$

Reexpressing the equation for n_{V_f} based on the modeling of the Stokes fall velocity in terms of $n_{d_{50}}$, Equation 4.8 and n_{V_f}, Equation 4.11,

$$n_{\gamma'} = \frac{\mu^{15/22}}{n_T^{9/11}} \tag{4.12}$$

For the modeling of H_o/V_fT,

$$n_T = \mu^{17/16} = \mu^{1.0625} \tag{4.13}$$

for the expressions of $n_{H_o} = \mu$ and n_{V_f}, Equation 4.11. Therefore, Equation 4.12 reduces to

$$n_{\gamma'} = \mu^{-0.1875} \tag{4.14}$$

and Equation 4.8 reduces to

$$n_{d_{50}} = \mu^{+0.063} \tag{4.15}$$

For the modeling of the horizontal velocity, $n_V = \lambda/n_T$. Substituting $n_V = \mu^{1/2}$ which models the Froude number and Equation 4.13 for n_T into the expression for n_V,

$$\lambda = \mu^{25/16} = \mu^{1.5625} \tag{4.16}$$

This model law scales both the grain size and the particle specific weight. For a small scale model, the model grain size would be smaller than the prototype but the specific weight would be larger.

5. Model Law #5

For the same material in the model and the prototype, $n_{\gamma'} = 1$, and for the same median diameter, $n_{d_{50}} = 1$, $n_{V_f} = 1$. Modeling H_o/V_fT,

$$n_T = \mu \tag{5.1}$$

Preserving the Froude number,

$$n_V = \mu^{1/2} \tag{5.2}$$

Modeling the horizontal velocity, V,

$$n_V = \frac{\lambda}{n_T} \tag{5.3}$$

Introducing the expressions for n_T and n_V,

$$\lambda = \mu^{3/2} \tag{5.4}$$

6. Model Law #6

Open channel flow can be represented by the Chezy equation as

$$V^2 = C_h^2 RS \tag{6.1}$$

where R, the hydraulic radius, equals the water depth, d, for wide channels and S, the slope of the channel bed, equals the change in vertical elevation per horizontal length. Defining the water depth, d, and the slope, S, in terms of λ and μ, the modeling of the Chezy equation yields

$$n_V^2 = n_{C_h}^2 \frac{\mu^2}{\lambda} \quad . \tag{6.2}$$

Modeling the Froude number, $n_V = \mu^{1/2}$, and introducing this expression into Equation 6.2,

$$n_{C_h}^2 = \frac{\mu}{\lambda} \quad . \tag{6.3}$$

The Chezy coefficient is defined as $C_h^2 = \frac{8g}{f}$. Modeling the Chezy coefficient, $n_{C_h}^2 = 1/n_f$ and substituting Equation 6.3 for n_{C_h},

$$n_f = \frac{\mu}{\lambda} \quad . \tag{6.4}$$

Modeling the bed shear velocity, u_*,

$$n_{u_*} = n_f^{1/2} n_V \quad . \tag{6.5}$$

Introducing $n_V = \mu^{1/2}$ per the modeling of the Froude number,

$$n_{u_*} = n_f^{1/2} \mu^{1/2} . \quad (6.6)$$

Substituting Equation 6.4 for n_f in Equation 6.6,

$$n_{u_*} = \frac{\mu}{\lambda^{1/2}} . \quad (6.7)$$

Preserving the bed.particle Reynolds number, $n_{u_*} = \frac{1}{n_{d_{50}}}$ and substituting this expression into Equation 6.7 for n_{u_*},

$$n_{d_{50}} = \frac{\lambda^{1/2}}{\mu} . \quad (6.8)$$

Per the preserving of the densimetric Froude number,

$$n_{u_*}^2 = n_{\gamma'} n_{d_{50}} . \quad (6.9)$$

Introducing Equations 6.7 and 6.8 into Equation 6.9,

$$n_{\gamma'} = \frac{\mu^3}{\gamma^{3/2}} \quad (6.10)$$

Substituting Equations 6.8 and 6.10 into the model expression for the Stokes fall velocity, $n_{V_f} = n_{d_{50}}^2 n_{\gamma'}$,

$$n_{V_f} = \frac{\mu}{\lambda^{1/2}} \quad (6.11)$$

Preserving $H_o/V_f T$,

$$n_T = \lambda^{1/2} . \quad (6.12)$$

For the same material in the model and the prototype, $n_{\gamma'} = 1$, Equation 6.10 reduces to

$$\lambda = \mu^2 \quad (6.13)$$

Equation 6.8 for $n_{d_{50}}$ reduces to $n_{d_{50}} = 1$ and Equation 6.12 for n_T reduces to

$$n_T = \mu . \quad (6.14)$$

7. Model Law #7

Preserving the wave steepness ratio, H_o/L_o,

$$\mu = \lambda \ . \tag{7.1}$$

For the same material in the model and the prototype, n_γ, = 1, and the same grain size, $n_{d_{50}}$ = 1, n_{V_f} = 1 and the modeling of H_o/V_fT yields $\mu = n_T$. In this case, however, the Froude number is not modeled.

Acknowledgements

This work was partially sponsored by the Office of Naval Research Geography Program.